atmosphere

MDPI

Article

Variation of Relative Humidity as Seen through Linking Water Vapor to Air Temperature: An Assessment of Interannual Variations in the Near-Surface Atmosphere

Jiawei Hao and Er Lu *

Key Laboratory of Meteorological Disaster, Ministry of Education (KLME), Joint International Research Laboratory of Climate and Environment Change (ILCEC), Collaborative Innovation Center on Forecast and Evaluation of Meteorological Disasters (CIC-FEMD), Nanjing University of Information Science and Technology, Nanjing 221000, China; 20181102033@nuist.edu.cn

* Correspondence: elu@nuist.edu.cn or lu_er@hotmail.com

Abstract: It has generally been regarded that, in the warming climate, atmospheric water vapor may increase due to the enhancement in surface evaporation, which is expected from the Clausius–Clapeyron (C–C) equation, along with the assumption that relative humidity experiences small changes. If the variation in relative humidity is small, the response of water vapor to temperature will be closely in line with the C–C equation. However, whether relative humidity experiences large or small changes needs be assessed, and the change of relative humidity should be compared with the change in surface–air temperature. In this study, we link surface vapor pressure, which characterizes atmospheric water vapor, to surface-air temperature, and treat both the temperature and relative humidity as influencing factors. A method based on linear regression is applied to compare the interannual variabilities of relative humidity and temperature in the interannual variation in surface vapor pressure. Whether the year-to-year perturbation of relative humidity is important, compared with the perturbation in surface-air temperature, is explored Results show that, at high latitudes of both hemispheres, the variation in vapor pressure is dominated by air temperature, and relative humidity has small positive contributions. Thus, the variation in relative humidity over these regions is comparably small, and the response of water vapor to temperature can well follow the C–C equation. Differently, at mid-low latitudes, especially on land, air temperature plays a negative role in the variation in vapor pressure. Relative humidity offsets the negative contribution and dominates the variation in vapor pressure, suggesting that the variation in the relative humidity over these regions is comparably large. Hence, the response of water vapor to temperature deviate from the C–C equation. Analysis indicates that the different results of the dominance from the two influencing factors are affected by the dual effects of precipitation or wet-air transport over land. Both precipitation and the transport of cold wet air could break the C–C relation between water vapor pressure and temperature.

Keywords: atmospheric water vapor; surface-air temperature; relative humidity; dominance analysis; interannual variations

Citation: Hao, J.; Lu, E. Variation of Relative Humidity as Seen through Linking Water Vapor to Air Temperature: An Assessment of Interannual Variations in the Near-Surface Atmosphere. *Atmosphere* **2022**, *13*, 1171. https://doi.org/10.3390/atmos13081171

Academic Editor: Yoshihiro Tomikawa

Received: 3 July 2022
Accepted: 21 July 2022
Published: 24 July 2022

1. Introduction

Atmospheric water vapor, a component in global water and energy cycle, is important to climate variability and change [1–3]. It is the material of precipitation, and the latent heat released from precipitation can drive atmospheric circulation [4]. The circulation may, in turn, transport water vapor and change the spatial distribution of the vapor [5]. As a greenhouse gas, water vapor can also affect the radiation in the atmosphere and the temperature of the Earth's atmosphere system [6].

Precipitable water (W), the column-integrated water vapor amount, is a conventional water vapor quantity. In a regional column, water vapor converging from the surroundings,

along with the moisture evaporated from earth's surface, is first used to increase the *W*. When the air gets saturated, at least in certain levels, precipitation may form. The data of *W* can be obtained from the sounding radiosonde [7,8], the remote sensing such as the radar observation and satellite retrievals [9,10], the GPS observations [11,12], and the calculations with the reanalysis and model outputs [13,14].

The surface water vapor, e.g., the surface vapor pressure, has also been stressed [15–18]. Surface vapor pressure can be regarded as the force exerted by the total moisture contained in the column [19]. It was revealed that, with a normal profile with water vapor content maximal in low level and decreasing with height, the surface vapor pressure can well represent the column total water vapor [20,21]. The empirical relations between *W* and surface vapor pressure were utilized to estimate *W* with surface observations, especially during the early stage when there were few sounding observations [22–25]. In the present study, while examining its relation with *W*, we focus on the interannual variation in surface vapor pressure. By linking the surface vapor pressure with precipitable water, we may analyze the interannual variability of surface water vapor to reflect that of the column-integrated water vapor content, which is meaningful for the main block of this study.

Because of warming, atmospheric water vapor is often linked to tropospheric temperature or surface-air temperature [26–29]. If the relative humidity that appears in the relation experience small changes, the response of vapor pressure to temperature follows the C–C equation, with a growth rate near 7%/K [30]. It seems to be true at global scale and in some local areas according to observations [31]. The response of global mean surface vapor pressure to temperature simulated by models are also close to it [32]. However, due to the limitation of evaporation and the variation in vapor transport, the relative humidity may have large changes in many areas [33]. There have been few studies on assessing the long-term changes, as well as the interannual variability, of the surface and tropospheric relative humidity. Some studies [16,34] examined the variability and trends in surface humidity using global in situ observations and pointed out that the interannual variations of the surface relative humidity are relatively small.

Actually, for the examination of how tightly the change of water vapor can follow the C–C equation, an assessment of whether the variation in relative humidity is large should be performed in the context of the variation in air temperature. In other words, the change of relative humidity should be compared with the change in air temperature. In this study, we link water vapor to the surface-air temperature and treat both the temperature and relative humidity as influencing quantities. The change in water vapor may be dominated by the change in air temperature or the change in relative humidity or be affected by both of them. For the interannual variation in the surface vapor pressure, which characterizes the atmospheric water vapor, we aim to explore whether the variation in air temperature or the variation in relative humidity is more important.

The physical expression of vapor pressure, air temperature, and relative humidity are nonlinear. A method is applied here, which has been utilized in previous studies for several different climate issues [35–38]. It uses linear regression to fit the relation, which is convenient for assessing the relative importance. Statistical tests are conducted to ensure the reliability of the method. In this study, with the two measures, constructed by using the coefficients from the fitting along with the standard deviations, the variations of air temperature and relative humidity in the interannual variation in vapor pressure are then estimated and compared. Finally, whether the variation in relative humidity is large and whether the response of water vapor to temperature can will follow the C–C equation can be explored.

In Section 2, the data and main method used in the paper are introduced. In Section 3, derivation and calculation are used to illustrate that surface vapor pressure can reflect the column-precipitable water under hydrostatic conditions. Section 4 shows the correlations of surface vapor pressure with surface-air temperature and relative humidity. In Section 5, a linear relation of surface vapor pressure with the two influencing factors is established by using statistical regression. In Section 6, the relative importance of the two factors in the

interannual variation in the vapor pressure is quantitatively assessed with the measures constructed from the fitting. In Section 7, the results of the dominance determined from the linear fitting method are compared with the conclusions qualitatively deduced from the original nonlinear relation. In Section 8, to better understand the dominance of the relative humidity in the variation in surface vapor pressure over mid-low-latitude land, the dual effects of the land precipitation on the surface moisture and air temperature are examined for selected areas. Summary and discussion are given in Section 9.

2. Data and Method

2.1. Data

The European Centre for Medium-Range Weather Forecasts (ECMWF) Reanalysis v5 (ERA5) dataset is utilized in the present study [39]. A version of the dataset with a resolution of $1^\circ \times 1^\circ$ in latitude and longitude is used in this study. The data used include the monthly mean precipitable water and the 2 m temperature (T) and dewpoint temperature over the 43 years from 1979 to 2021. The near-surface vapor pressure (E), saturation vapor pressure (e_s), and relative humidity (R) are computed from the data. After translate the T into Celsius temperature scale, the vapor pressure and saturation vapor pressure are calculated with a modified Tetens formula, which is

$$e_s = 6.112exp(\frac{17.67T}{T+243.5}). \quad (1)$$

Calculations and plots are performed for all 12 months, and results of 4 months, including January, April, July, and October, are presented. While using the precipitation of this reanalysis, we also utilize the monthly precipitation from the CPC (Climate Prediction Center) Merged Analysis of Precipitation (CMAP) [40], which has a horizonal resolution of $2.5^\circ \times 2.5^\circ$.

2.2. Method

In the physical expression of vapor pressure, air temperature and relative humidity are nonlinearly linked, which is

$$E = e_s(T) \cdot R. \quad (2)$$

A method is applied here, which has been utilized in our previous studies for several different climate issues [35–38]. It uses linear regression to fit the relation between surface vapor pressure, temperature, and relative humidity as

$$E = AT + BR + C. \quad (3)$$

For the general nonlinear relation $E = E(T, R)$, we use the linear regression to fit it. The regression equations at all grids can pass the 0.01 significance level of the F-test. The coefficients obtained from the fitting, and the correlation between the two influencing factors are presented. The meaning of the regression coefficients A and B, through expressing them as $A = \partial E/\partial T$ and $B = \partial E/\partial R$, is that they stand for, respectively, the change rates of E with respect to T and R.

The standard deviations σ_T and σ_R can reflect the scales of the year-to-year perturbations of T and R. Then, we construct the two measures $S_T \equiv |\partial E/\partial T| \cdot \sigma_T$ and $S_R \equiv |\partial E/\partial R| \cdot \sigma_R$, the products of the change rates and the perturbation scales, to estimate the contributions of T and R to the variation in E. With the coefficients A and B fitted from the regression, the two measures can finally be expressed as

$$S_T = |A| \cdot \sigma_T \text{ and } S_R = |B| \cdot \sigma_R. \quad (4)$$

The two measures are calculated here to estimate the contributions of T and R to the interannual variation in E and compare their relative importance. The method is convenient for assessing the relative importance. Statistical tests of the regression are conducted to

ensure the reliability of the method. In this study, with the two measures, constructed by using the coefficients from the fitting along with the standard deviations, the contributions from the air temperature and relative humidity in the interannual variation in the vapor pressure are then estimated and compared.

3. Relating the Column-Integrated Water Vapor to the Surface Vapor Pressure

Precipitable water W is the column-integrated water vapor content and is expressed as $W = \int_0^\infty (q\rho)dz$, where q is specific humidity, and ρ is air density. Assuming the atmosphere is in hydrostatic balance, we may use a pressure coordinate and express it as $W = \int_0^{p_s} (q/g)dp$, where the surface pressure p_s may vary with time and location, and the gravitational acceleration g can be treated as a constant.

The sigma coordinate $\sigma \equiv p/p_s$ can be used, and the specific humidity can be expressed as $q = \varepsilon e/p$, where e is vapor pressure, and ε is the ratio of the gas constants for dry air to water vapor. As presented in [21], the W can be converted into the following novel form

$$W = (\varepsilon/g)\int_{\sigma=0}^{\sigma=1} e \cdot d(\ln \sigma). \tag{5}$$

The vapor pressure e normally has its maximum at the surface and decreases exponentially with the height to zero [41]. Hence, the vapor pressure can be treated as a function of σ, and an expression $e = E \cdot \sigma^n$ is assumed, and n is a constant, which may vary with the location. After the integration in (4), we finally obtain

$$W = k \cdot E, \tag{6}$$

where $k = \varepsilon/(gn)$. Equation (6) shows that, as suggested in [21], W can be estimated with the surface vapor pressure E.

There are two advantages for using the sigma coordinate. One is that, with the expression (6), the change of the W between two atmospheric states, both temporal and spatial changes of different scales, can be conveniently calculated. In the conventional expression with the pressure coordinate, the surface vapor pressure p_s varies with time and location. The second advantage is that, with the relation (6), the surface quantities can thus be introduced. As will be explained below, when stressing the response of water vapor to temperature, W may be further linked to the surface-air temperature.

The linkage of the precipitable water W with the surface vapor pressure E can be understood from the physical concept that the surface vapor pressure can be regarded as caused by the total water vapor contained in the vertical column, similar to the surface pressure being caused by the mass of the air column. Here, the condition for the linkage is that the atmosphere is stable and in hydrostatic balance. As mentioned above, due to practical needs in an early stage, W has been estimated with the data of surface vapor pressure and dewpoint temperature [22,23]. In turn, over oceans, surface humidity may also be inferred from the satellite-observed W [24].

Figure 1 shows the distributions of the correlation between W and surface vapor pressure E. At the monthly scale, from the globe, the interannual variations in W can be well represented by the surface vapor pressure. The representation is relatively poor in the tropics, where the atmosphere may be less stratified and may have more convection. The areas with insignificant correlation between W and E are much smaller in January than in July. The positive correlations are significant and strong over the high latitudes of the two hemispheres for January, April, and October. The correlations can be particularly strong over land in the mid-high latitudes, e.g., in January, the Antarctic region, Australia, the Eurasian continent, Greenland, and the North America. In July, over the high latitudes of northern hemisphere, the correlations are strong over the land of the Eurasian continent, Greenland, and the North America, while the correlations are insignificant over many of the regions that are immediately off the coast of these lands.

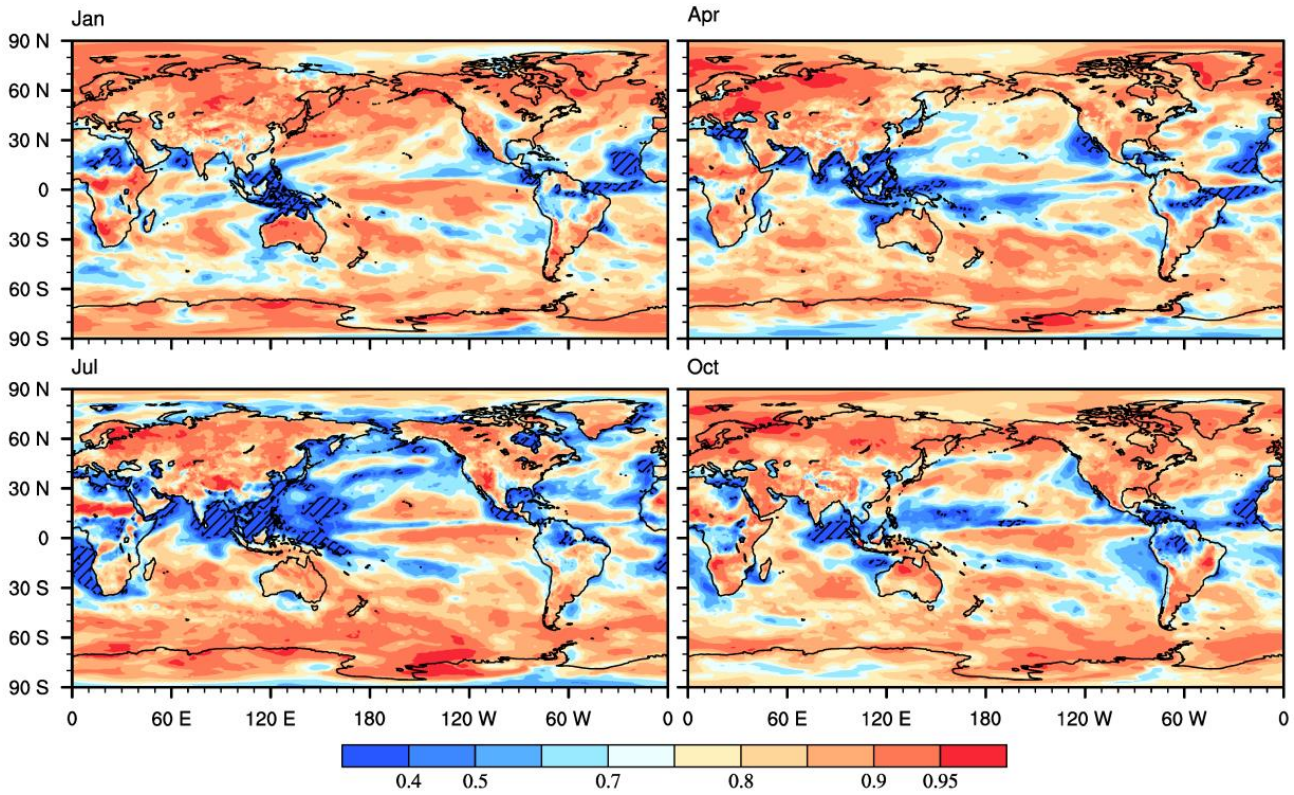

Figure 1. Distributions of the correlation coefficient between W and surface vapor pressure E, calculated with monthly data from 43 years. The areas where the correlation is not significant at the 0.05 level are marked with diagonal lines.

4. Variation in Surface Vapor Pressure with Air Temperature and Relative Humidity

The water capacity of air is only reflected by temperature. Furthermore, the water vapor contained in the near-surface air may significantly be contributed from, and thus be affected by, surface evaporation. Because of this, surface vapor pressure E is usually linked to surface-air temperature T through the expression of the saturation vapor pressure.

In the interannual variation in E, if relative humidity R is constant or does not change much, then we may estimate the vapor pressure from the air temperature. A large year-to-year perturbation of R may destroy the tightness of the relation between E and T. Whether the variation in R, over different areas, is large or small should be compared with the variation in T. Thus, in addition to the air temperature, relative humidity is also treated as an influencing factor. We could consider the synergistic influences of T and R and compare their relative importance.

Figure 2 shows the distributions of the correlation between surface vapor pressure E and surface-air temperature T. In the Southern hemisphere, positive correlations are strong in high-latitude regions, especially the Antarctic area, for all months. In the Northern hemisphere, positive correlations are also strong in high-latitude regions, including both the land and the Arctic Ocean, in January, April, and October. The correlations in July are less strong. Over the tropics and low latitudes, the correlations are, in general, weak or negative. Over tropical oceans, correlations are generally insignificant. The correlations can be significant and negative over many of the land areas, e.g., in January, over Australia, South Africa, and part of South America.

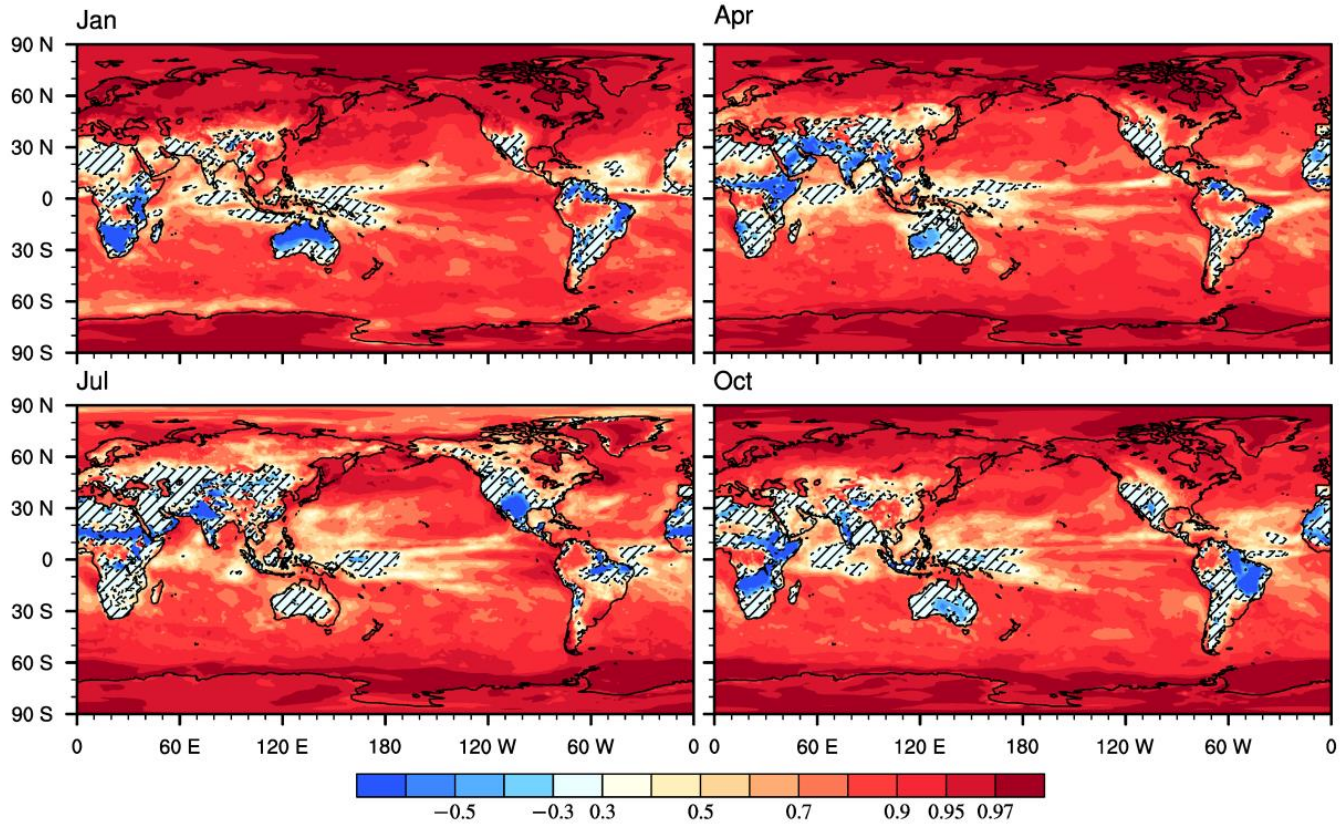

Figure 2. As in Figure 1 but between surface vapor pressure *E* and surface-air temperature *T*.

Figure 3 shows the distribution of the correlation between surface vapor pressure and the surface relative humidity. Overall from the globe, correlations are positive and can be significant. The spatial patterns of the correlation seem to be geographically affected. The correlations are particularly strong over land, e.g., Australia, South Africa, as well as the southern part of Eurasia and North America, for all months. The regions where the correlations are insignificant are generally in narrow belts. For example, the belts appear north of the Antarctic in April, July, and October, and this may be related to the Southern Annular Mode [42]. The region of the insignificant correlation appears over the tropical western Pacific Ocean, and this may be related to the sea surface temperature pattern of the El Niño–Southern Oscillation (ENSO) [43]. At mid-high latitudes in northern hemisphere, the areas with insignificant correlations may appear in the middle of continents or coastal regions. These belts with the insignificance of the relative humidity in influencing the surface vapor pressure act to separate the regions over the globe, and these regions may fundamentally belong to different atmospheric circulation regimes.

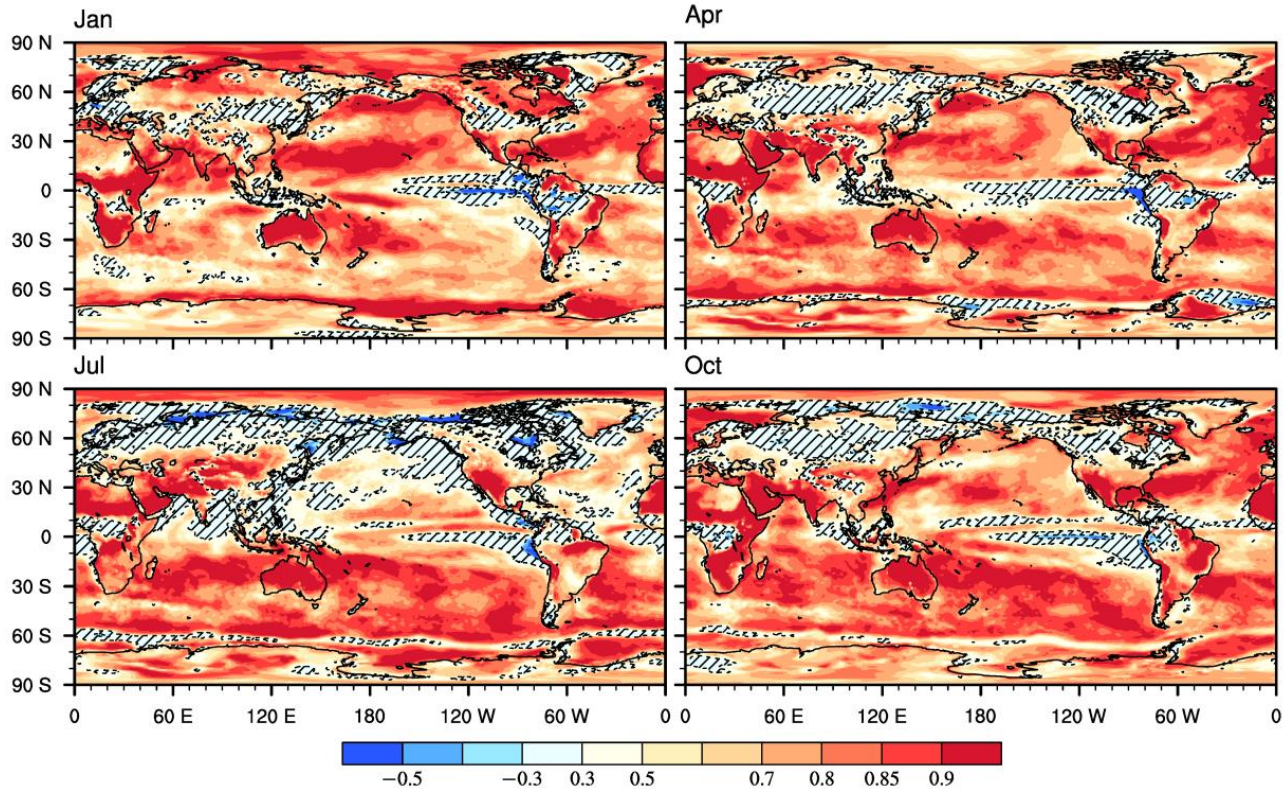

Figure 3. As in Figure 1 but between surface vapor pressure E and surface-air relative humidity R.

5. The Linear Fitting of Surface Vapor Pressure with the Two Influencing Quantities

The relation of E with two influencing factors T and R, as in Equation (2), is nonlinear, and it may generally be written as $E = E(T,R)$. Previous studies show that, for many issues, the relations can be linearized, which makes it convenient to estimate the relative importance of the influencing quantities [36,37]. Herein, we use linear regression to fit the relation. With the data collected and calculated from the three quantities, the coefficients A and B, as well as the constant term C, are determined from the fitting. For the nonlinear issue, statistical test is required to ensure the validation of the linearization.

The distributions of the correlation between the E calculated with reanalysis data and the E regressed with the linear relation are compared (figures are not shown). In most of the globe, the coefficient of the multiple correlation can be over 0.99. In some areas in the high latitudes of the two hemispheres, the correlations are relatively weaker but still can be greater than 0.90. The reason might be that in Equation (2), E is directly proportional to e_s but not T. As a test, to compare with relation (3), a linear regression is also performed to link E to R and e_s rather than T. Then the corresponding multiple correlation coefficient can be over 0.99 in all of the grid points. We also conducted F tests for the coefficients of the regression, and results show that the tests are significant at a 95% confidence level for all the grid points (figures not shown). These suggest that the fitting for the issue is robust and that the linearization is perfect everywhere in the globe. The feasibility of the linearization may be due to the special form of the nonlinear relation (2). That is, the variable E is a function increasing with respect to both T and R.

Figure 4 shows the distributions of the coefficients A and B calculated from the data with linear regression. The coefficient A of surface-air temperature T and the coefficient B of relative humidity R are similar in spatial patterns. They are both positive, maximal over the tropics, and decrease with latitude. In the plot of B for January, at high latitudes in the Northern hemisphere, while relatively the value is slightly positive in most of the region, there are some small areas where the values are small and negative, and this may be due to the computational reason for the relative humidity.

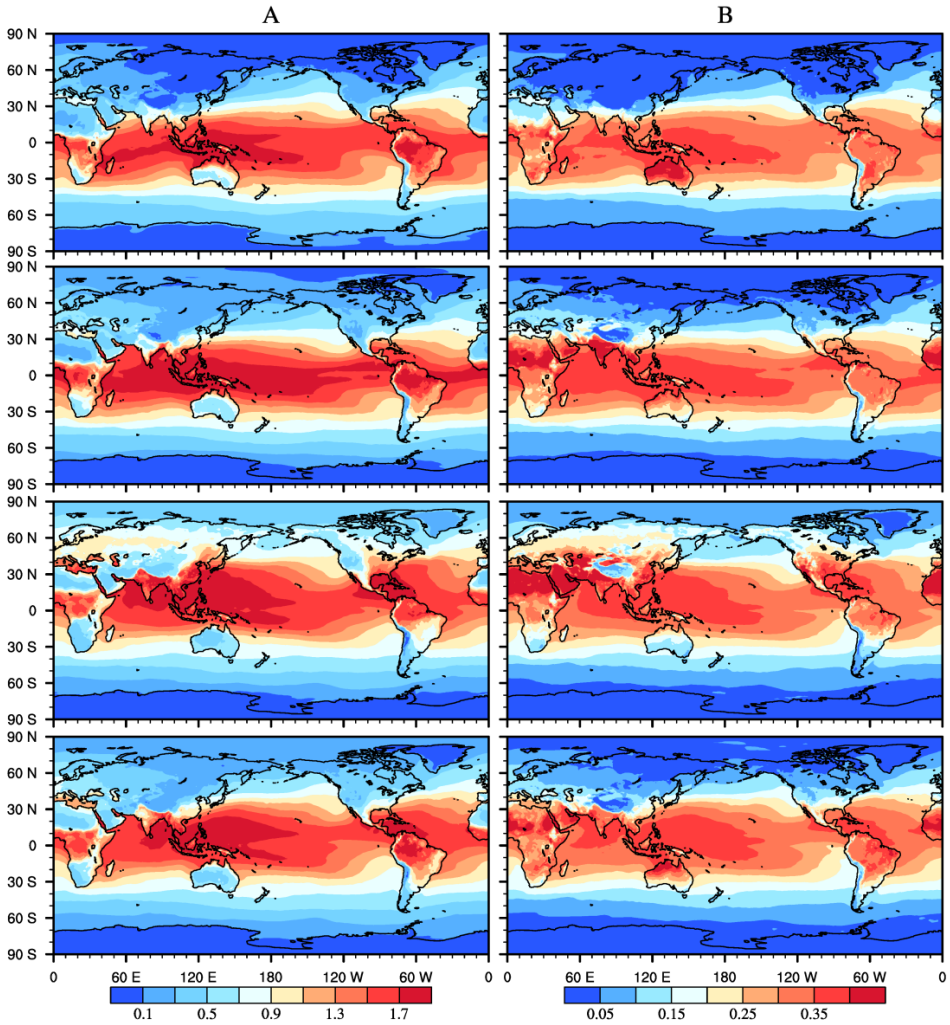

Figure 4. Distributions of the coefficients A (**left**; hPa/K) and B (**right**; hPa/%) obtained with the linear regression. The rows from top to bottom are correspond to January, April, July, and October respectively.

The meaning of the coefficients A and B can be better interpreted through expressing them in terms of the correlation coefficients and standardized deviations. As derived in [37], the coefficients can be expressed as

$$A = \widetilde{r}_{ET}\sqrt{\frac{1-{r_{ER}}^2}{1-{r_{TR}}^2}}\left(\frac{\sigma_E}{\sigma_T}\right) \text{ and } B = \widetilde{r}_{ER}\sqrt{\frac{1-{r_{ET}}^2}{1-{r_{TR}}^2}}\left(\frac{\sigma_E}{\sigma_R}\right), \tag{7}$$

where $\widetilde{r}_{ET}$ and $\widetilde{r}_{ER}$ are, respectively, the partial correlations of E with T and R. Two coefficients r_{ET} and r_{ER} are corresponding simple correlations, and σ_E, σ_T, and σ_R are standard deviations of the three quantities. These expressions suggest that the coefficients A and B of the linear regression proportionally link to the partial correlations, not the simple correlations.

Figure 5 shows the distributions of correlation coefficient between two influencing factors, the surface-air temperature T and the relative humidity R. Overall, in the globe, these two quantities can be independent and have significant positive or negative correlations, depending on the region. The spatial pattern of the correlation shows a seasonal change. The distributions in January, April, and October are similar. The correlation of T and R is significant and negative at mid-low latitudes, especially over land and tropical oceans. The correlation can be significant and positive over the Arctic and Antarctic regions. Over the middle latitudes of both hemispheres, the correlation is not significant. For July, negative correlation mainly appears in the Northern hemisphere. Over the Southern hemisphere and Greenland, the correlation can be positive.

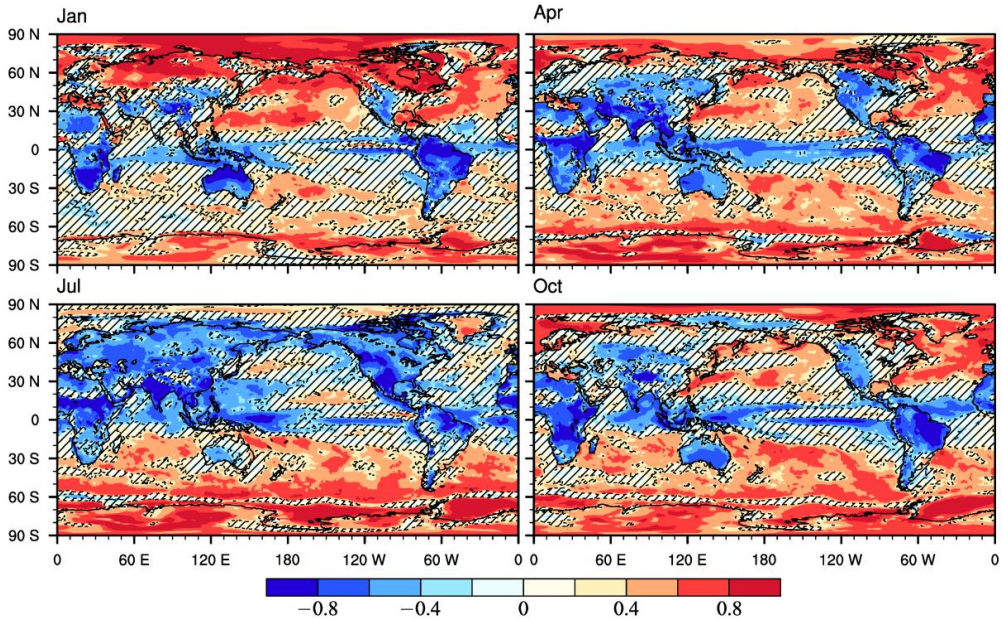

Figure 5. Distributions of the correlation coefficient between surface-air temperature T and relative humidity R.

As will be analyzed in Section 7, Equation (2) can be used to qualitatively examine the effects of the two influencing quantities. For the positive correlation of T and R over mid-high latitudes, they may both have positive contributions to the variation in E. However, whether T or R is more important needs to be further assessed. Differently, for the two quantities that have negative correlation over the mid-low latitudes, one of them may have a positive contribution to the variation in E, while the other may have a negative contribution. When they are negatively correlated, T and R may offset each other. However, whether T or R dominates the variation in E may be uncertain, and this will be determined with the data.

The coefficients A and B, as mentioned above, directly link to the partial correlations. For study, we may qualitatively examine the partial correlations from the original physical relation $E = R{\cdot}e_s(T)$. Taking T as a constant, then E is proportional to R, so the partial correlation of E with R should be 1. When taking R as a constant, the partial correlation of E with e_s should also be 1, whereas the partial correlation with T may not be able to reach 1, but it can be expected to be rather strong and very close to 1. By using the data of the three quantities, two partial correlations are calculated. Results show that the partial correlation of E with R can be over 0.99 everywhere in the globe (figures are not shown). The partial correlation of E with T can be up to 0.99 almost across the entire field. It is slightly weaker in some high-latitude areas in the winter hemisphere (figures are not shown).

6. The Dominance of the Two Factors in the Variation in Surface Vapor Pressure

For different nonlinear problems, a simple method was designed, through linear fitting, and applied to estimate the contributions and their relative importance in the influencing quantities in our previous studies [35–37]. For the general nonlinear relation $E = E(T,R)$, we use the linear regression $E = AT + BR + C$ to fit it.

The meaning of the coefficients A and B, through expressing them as $A = \partial E/\partial T$ and $B = \partial E/\partial R$, is that they stand for, respectively, the change rates of E with respect to T and R. The standard deviations σ_T and σ_R can reflect the scales of the year-to-year perturbations of T and R. Then, we construct the two measures $S_T \equiv |\partial E/\partial T| \cdot \sigma_T$ and $S_R \equiv |\partial E/\partial R| \cdot \sigma_R$, the products of the change rates and the perturbation scales, to estimate the contributions of T and R to the variation in E. The two measures are calculated here to estimate the contributions of T and R to the interannual variation in E and to compare their relative importance.

For surface-air temperature, standard deviation is small over the mid-low latitudes and is large over the mid-high latitudes of both hemispheres (figures not shown). The deviations over the Arctic region and Antarctic region show significant seasonal variations. The maximal standard deviation of surface temperature appears in the high latitudes in winter hemisphere. For surface relative humidity, the standard deviation is small over the oceans and is large over the land of most continents, including Australia, Africa, Eurasia, North America, and South America. The deviation is not large over the Antarctic and Greenland, and this may be related to the snow cover there. Compared with the temperature, the deviation in relative humidity does not tend to vary with latitude.

Figure 6 shows the distributions of S_T and S_R, the relative contributions from surface-air temperature and relative humidity. From their spatial patterns, the surface water vapor E and its year-to-year perturbation σ_E are both maximal over the tropics and decrease with latitude (figures not shown). According to Equations (4) and (7), the contributions S_T and S_R both have the magnitude of σ_E. Thus, in Figure 6, S_T and S_R are both large over the mid-low latitudes and small over the high latitudes. Their large-value belts both shift seasonally, from a relatively southern position in January to the northern position in July. Comparably, the contribution from relative humidity is larger than that from temperature over mid-low latitudes, especially over land.

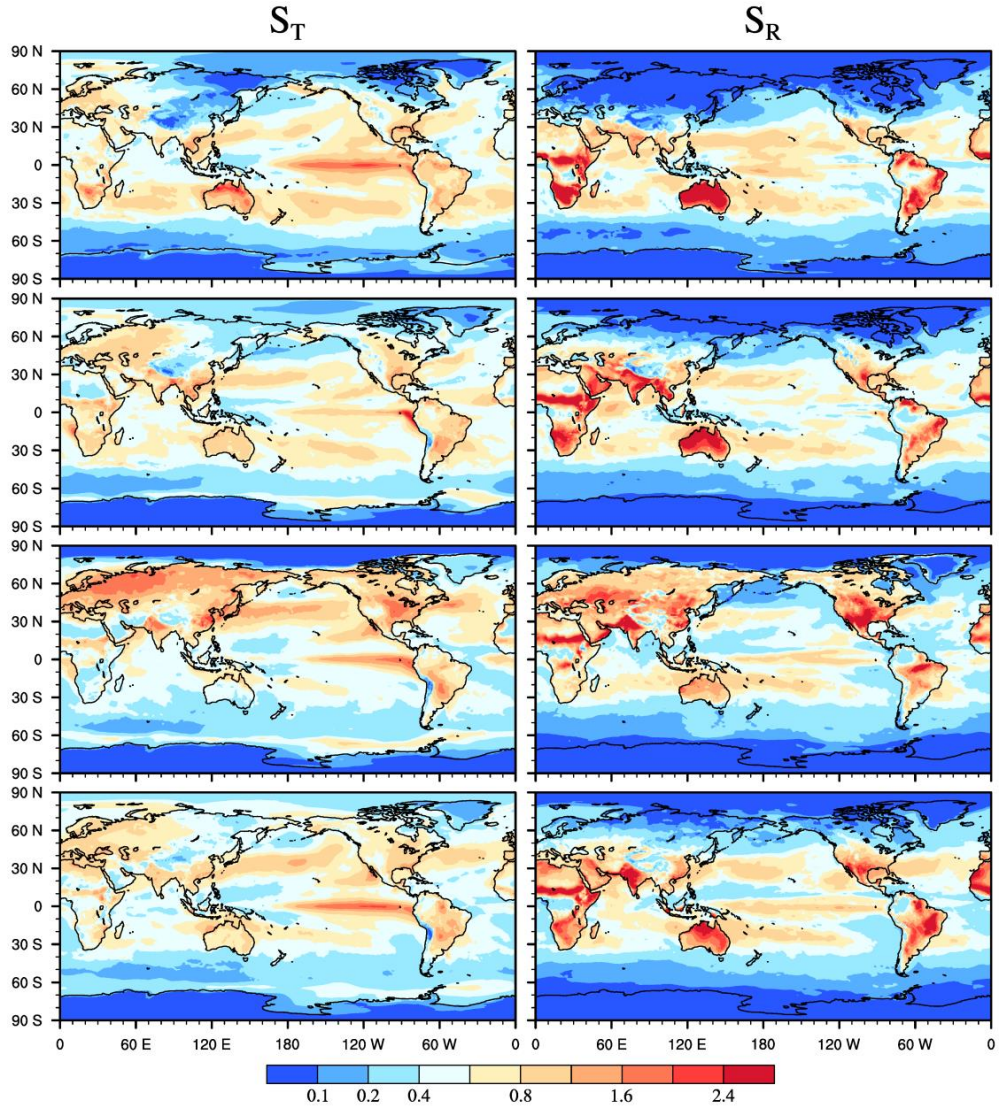

Figure 6. Distributions of the S_T and S_R. The unit is hPa. The rows from top to bottom are correspond to January, April, July, and October respectively.

Figure 7 shows the distribution of $S_R - S_T$, the difference between contribution from surface relative humidity and that from surface-air temperature, which reflects the relative importance of the two influencing quantities. It is revealed that surface relative humidity can dominate the interannual variation in surface vapor pressure over mid-low latitudes. The dominance is strong over land, including Australia, Africa, South Asia, South America, and the southwest portion of the United States. The dominance of relative humidity also prevails over oceans, including the north Indian Ocean, the tropical western Pacific Ocean, and the tropical Atlantic Ocean. By contrast, surface-air temperature dominates the variation in surface vapor pressure over the mid-high latitudes of both hemispheres. The dominance can be strong in some of the areas there.

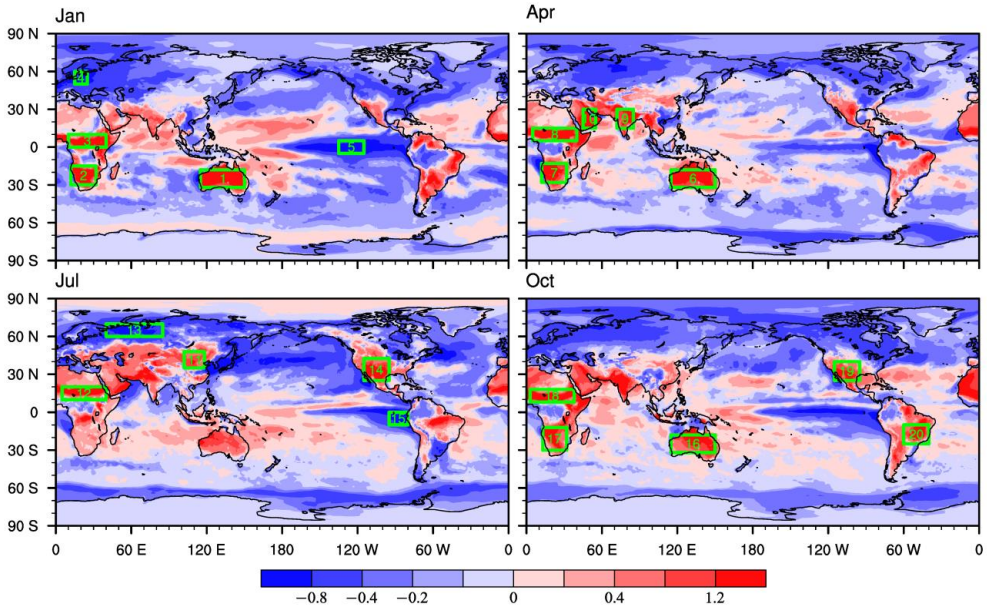

Figure 7. Distribution of the difference from $S_R - S_T$. The unit is hPa. The 20 areas, with 5 for each of the four months, are major positive (red) and negative (blue) centers and are selected for use in Section 8 and Table 1.

Table 1. The interannual correlations between the precipitation P and surface vapor pressure E (r1), the P and surface-air temperature T (r2), the E and T (r3), and the E and surface relative humidity R (r4). These quantities are averaged over the 20 areas selected in Figure 7 for the four months. For the 43-year variations, the correlation coefficient at the 0.05 significance level is 0.294. The values of the precipitation averaged over the area and over the month of the 43 years (P, mm/day) are also provided. For precipitation, while using the ERA5 reanalysis, the CMAP data is also utilized. In the columns of r1, r2, and P, the results from the CAMP precipitation are given in parentheses. The correlations that are significant at the 0.05 level are highlighted in bold font. The serial number of two oceanic areas are marked as blue and those of the two high-latitude areas are marked as red.

Serial Number	r1 (P, E)	r2 (P, T)	r3 (E, T)	r4 (E, R)	P
1	**0.82 (0.87)**	**−0.46 (−0.44)**	−0.24	**0.92**	2.09 (2.25)
2	**0.95 (0.93)**	**−0.78 (−0.82)**	**−0.71**	**0.95**	3.71 (3.23)
3	**0.90 (0.74)**	−0.15 (0.07)	0.17	**0.90**	0.88 (0.79)
4	−0.07 (−0.09)	**0.31 (0.39)**	**0.99**	0.13	1.74 (2.27)
5	0.14 (0.16)	**0.71 (0.65)**	**0.97**	−0.04	1.95 (1.36)
6	**0.87 (0.89)**	**−0.57 (−0.52)**	−0.16	**0.89**	0.73 (0.76)
7	**0.88 (0.86)**	−0.25 (−0.25)	−0.09	**0.92**	0.98 (1.10)
8	**0.89 (0.77)**	**−0.70** (−0.20)	−0.21	**0.92**	1.81 (1.81)
9	**0.80 (0.85)**	**−0.67 (−0.60)**	0.04	**0.83**	0.43 (0.53)
10	**0.82 (0.91)**	**−0.50 (−0.54)**	−0.19	**0.88**	0.20 (0.44)

Table 1. *Cont.*

Serial Number	r1 (*P*, *E*)	r2 (*P*, *T*)	r3 (*E*, *T*)	r4 (*E*, *R*)	*P*
11	**0.53 (0.48)**	**−0.72 (−0.62)**	**0.98**	**−0.45**	6.42 (7.14)
12	**0.90 (0.72)**	**−0.81** (−0.30)	−0.38	**0.87**	2.49 (3.02)
13	**0.77 (0.76)**	−0.33 (−0.26)	**0.92**	−0.3	2.29 (2.19)
14	**0.84 (0.75)**	**−0.64 (−0.48)**	−0.22	**0.78**	1.85 (2.11)
15	−0.37 (−0.29)	**0.62 (0.59)**	**0.98**	**−0.42**	0.29 (0.14)
16	**0.94 (0.95)**	**−0.63 (−0.59)**	−0.29	**0.89**	0.47 (0.55)
17	**0.90 (0.84)**	**−0.66 (−0.59)**	**−0.49**	**0.93**	1.01 (0.90)
18	**0.92 (0.76)**	**−0.43** (0.14)	0.20	**0.89**	1.33 (1.45)
19	**0.90 (0.89)**	**−0.59 (−0.53)**	−0.10	**0.87**	1.44 (1.45)
20	**0.87 (0.77)**	**−0.73 (−0.57)**	−0.33	**0.80**	3.95 (3.90)

7. Comparison with the Qualitative Deduction from the Original Nonlinear Relation

The original physical relation (2) is nonlinear and cannot conveniently provide quantitative results for the dominance. Hence, the linear fitting method is used. For this method, although quantitative results can be archived, since it is statistically based, we hope that the results could still be verified. On the other hand, for the original physical relation, although it is nonlinear, it is special in the form of the function, with E varying with each of T and R as a monotonically increasing function. Hence, we may deduce qualitatively the relations of E with each of T and R. Then, with aid of the correlation between two influencing quantities T and R, some qualitative conclusions may be deduced from the nonlinear physical relation. A comparison shows that the quantitative results of the dominance determined from the linear fitting method can be supported by the conclusions qualitatively deduced from the nonlinear physical relation.

At mid-high latitudes of both hemispheres (except for the Northern hemisphere in July), with the variations in January over the Arctic region being an example, as revealed from the data, the two influencing quantities T and R are positively correlated ($r_{TR} > 0$; Figure 5). Corresponding to this, Figure 2 shows that T in this region has a strong positive correlation with E ($r_{ET} > 0$), and Figure 3 shows that overall R may have a positive correlation with E ($r_{ER} > 0$). From the physical relation $E = R{\cdot}e_s(T)$, T and R both have positive relations with E, and thus both have positive contributions to the variation in E. However, for further analysis, whether T or R contributes more and thus is more important in the variation in E cannot be identified from this physical relation. Instead, we need to use the linear fitting method to quantitatively determine the dominance. Figure 7 illustrates that, for this situation, e.g., over the Arctic region for January, the variation in E is dominated by T. This suggests that the interannual variation in the surface relative humidity over the mid-high latitudes is comparably small.

Over the mid-low latitudes, especially over land, the two influencing quantities T and R are negatively correlated ($r_{TR} < 0$; Figure 5). The variations in January over Australia are an example. Correspondingly, Figure 2 shows that, over this region, T has a negative correlation with E ($r_{ET} < 0$), suggesting that E does not increase with T. Figure 3 shows that R has a positive correlation with E ($r_{ER} > 0$). From the physical relation, $E = R{\cdot}e_s(T)$, we can infer that, because of the negative effect from T, R should have a strong positive relation with E, which can offset the negative effect of T. For this situation, the dominance of these two quantities can be qualitatively deduced from the original nonlinear physical relation. By using the linear fitting method, the results for the dominance can be quantitatively determined. A comparison indicates that the qualitative deduction supports the quantitative results. Figure 7 demonstrates that, in this case, e.g., in January over Australia, the variation in E is truly dominated by R. Thus, the interannual variation in the surface relative humidity over mid-low latitudes is comparably large.

8. The Dual Effects of Precipitation on the Dominance of Surface Vapor Pressure over Land

The above analyses indicate that, over land at mid-low-latitude, surface vapor pressure does not follow surface-air temperature, in their interannual variations, as reflected in Figure 2. The surface relative humidity may have, relatively, large interannual variations and thus dominate the variation in surface vapor pressure, as illustrated in Figure 7. To better understand this issue, in this section, we examine the effects of precipitation over land through regional analysis.

In Figure 7, we select 20 areas, with 5 for each of the four months. These areas cover the major positive and negative centers of $S_R - S_T$ over the globe. There are, in total, for the four months, 16 land areas at mid-low latitudes. For comparison, we also include 2 land areas at high latitudes (Area 4 and 13) and 2 ocean areas in the tropics (Area 5 and 15). The precipitation, surface vapor pressure, surface-air temperature, and surface relative humidity are averaged over each of the areas, for the different months, while the averaged relative humidity is calculated with the averaged E and e_s.

Table 1 presents the 43-year average of precipitation (P), as well as the interannual correlations between P and E (r1), P and T (r2), E and T (r3), and E and R (r4). For the data on precipitation, while using the ERA5 reanalysis, we also utilize the CMAP analysis. The results from the CMAP data are provided in parentheses. Comparisons show that, for the 20 areas, the values of precipitation P obtained from the two datasets are consistent in magnitude. The values for each of the correlations r1 and r2 with the two datasets are, overall, rather consistent both in sign and in magnitude.

The precipitation over land at mid-low latitudes may have dual effects. One is to influence the surface vapor pressure. In rainy years, the wet land surface may lead to more evaporation from the surface, which can help the near-surface air obtain more moisture. It is shown in Table 1 that the correlations of precipitation with surface vapor pressure (r1) are positive over all of the 16 land areas at mid-low latitudes, for both precipitation datasets. The correlation is significant, at a 95% confidence level, for all of the 16 areas with both precipitation data.

The other effect of land precipitation is to influence surface-air temperature. In rainy years, since more energy received by the surface is consumed for evaporation, there is less energy left behind, as sensible heat to warm the air, which may lead to a lower surface-air temperature. Among the 16 land areas at mid-low latitudes, as shown in Table 1, the correlations of precipitation with surface-air temperature (r2) are all negative in ERA5 datasets, and there are 14 negative correlation areas for CMAP precipitation data. The negative correlation is significant for 14 areas with the ERA5 precipitation and 11 areas with the CMAP precipitation. There is only one area (area 3) where the precipitation and the surface-air temperature have a positive correlation, but it is not significant for either precipitation dataset.

As a result of the dual effects from the land precipitation, i.e., the precipitation can increase the near-surface moisture but lower the air temperature, the surface vapor pressure and surface-air temperature may tend to be negatively related. Among the 16 land areas, in Table 1, the correlation r3 is negative for most areas. The negative correlation is significant in Area 2, 3, 8, 12, 17, and 20. Thus, over mid-low-latitude land, the effects of the precipitation make the surface vapor pressure and surface-air temperature disobey the Clausius–Clapeyron equation.

The preference of the negative relation between E and T controlled by precipitation implies that, from the physical relation $E = R \cdot e_s(T)$, surface relative humidity R can be positively related with surface vapor pressure E and thus dominates the variation in E. Table 1 shows that the correlation of surface vapor pressure with relative humidity (r4) is over 0.80 in all of the 16 areas and is over 0.90 in 12 areas. The correlations of surface vapor pressure with relative humidity are much stronger than its correlations with the air temperature in magnitude. These results suggest that the surface relative humidity, as reflected by its dominance, may have relatively large interannual variations over mid-low-latitude land.

For the two areas on land at high latitudes, Area 4 and 13, Table 1 shows that the precipitation on land has less influence on surface vapor pressure and air temperature. Unlike mid-low-latitude lands, the surface vapor pressure in high-latitude land areas has strong positive correlations with air temperature, and, correspondingly, the surface relative humidity can remain interannually stable. For the two areas in tropical oceans, Area 5 and 15, the correlations r1 and r2 are all positive and strong. While precipitation over the ocean may have certain influence on the surface-air temperature, it is more likely that precipitation is the result of surface vapor pressure and air temperature and thus can indicate their variations. The surface vapor pressure over ocean areas has positive and strong relations with surface-air temperature. Although surface relative humidity also has contributions, the variations in surface vapor pressure are dominated by surface-air temperature.

9. Summary and Discussion

9.1. The Linkage between Precipitable Water and Surface Vapor Pressure

Water vapor is important to precipitation and climate change. Water vapor content is generally maximal at near-surface level and decreases with altitude. The surface vapor pressure and the precipitable water, the column-integrated water vapor, are two quantities commonly used for assessing the moisture condition of the atmosphere. In this study, we focus on the interannual variation and explore whether surface vapor pressure can reflect the precipitable water firstly. If the interannual variations in precipitable water and surface vapor pressure are consistent, the response character of surface vapor pressure to the temperature can reflect that of the column water vapor content.

The surface vapor pressure can be used to represent precipitable water in many areas. By using a sigma coordinate, the vertical integration for calculating W can be easily linked to a surface quantity, i.e., the surface vapor pressure. We thus establish the simple relation between W and E. The condition for the relation is that the atmosphere is in hydrostatic balance, and it is stratified with no convection. The physical basis for the linkage is that the surface vapor pressure is the force exerted on the surface by the total water vapor contained in the vertical column. Results show that the correlations of monthly W and E are positive and significant over most of the areas in the globe, especially at the mid-high latitudes of both hemispheres. The relation is weak in some tropical ocean areas and, in boreal summer, some areas at high latitudes. In most areas out of tropics, the interannual variation in surface vapor pressure can well reflect that of precipitable water.

9.2. The Response of Vapor Pressure to Temperature

How tightly the surface vapor pressure can be linked to the surface-air temperature, as well as whether the interannual variation in relative humidity is high when compared with the interannual variation in surface-air temperature, is explored. Surface vapor pressure is generally linked to surface-air temperature due to saturated water vapor pressure. When linking E to the temperature, the expression contains surface relative humidity. If R does not change much, one may use surface-air temperature and the C–C relation to estimate E under global warming. If the variation in R is large, E may not well follow the variation in surface-air temperature. In the variation in vapor pressure, whether R has a large or small variation needs to be assessed by comparing it with the variation in T. Thus, relative humidity is treated as an influencing quantity. Then the synergistic influences of T and R are examined, and their contributions are estimated, to determine the dominance of these two quantities in the interannual variation in surface vapor pressure.

The original physical relation is nonlinear, and it cannot be used directly to quantitatively determine the relative importance. Statistical fitting is then used to linearize the relation. A significance test shows that the fitting is robust and that the regression effect is perfect everywhere in the globe. In general, two influencing factors T and R, as revealed from the data, may have different relations. They can be independent, positively

or negatively correlated. Nevertheless, two coefficients in the linear fitting are linked to the partial correlations, not the simple correlations, of E with T and R.

The relative importance of the two influencing factors is finally determined from two measures that are constructed with the coefficients of linear fitting. The results of the dominance estimated with the linear fitting method show that surface-air temperature dominates the interannual variation in surface vapor pressure at mid-high latitudes and that the surface water vapor can follow the temperature close to the C–C equation. Surface relative humidity dominates the variation in vapor pressure at mid-low latitudes, especially on land, and the relation between surface water vapor and temperature tends to deviate from the C–C equation.

The linear fitting method can provide quantitative results, and the method has been applied in our previous studies for the dominance analysis. However, we still hope that the reliability of the results could be verified. The original physical relation, in spite of the nonlinearity, is simple and special as a function. From the physical relation, we can deduce some qualitative statements for dominance. A comparison shows that these statements can support the results obtained from the statistical method. At mid-high latitudes, based on the positive correlation of two influencing factors calculated from the data, the physical relation suggests that T and R both have positive contributions to the variation in E. At mid-low latitudes, with the negative correlation between T and R, it can be inferred from the physical relation that, when E decreases with T, the E must have a strong positive relation with R, thus R dominates the variation in E.

Precipitation is introduced to understand the dominance of surface relative humidity in the variation in surface vapor pressure on land at mid-low latitude. Calculations reveal that the precipitation on land exhibits dual effects. One is to increase the surface vapor pressure. The other is to decrease the surface-air temperature. In rainy years, besides the direct cooling effect of precipitation, since more energy is consumed for evaporation, there is less sensible heat left to warm the air, which may lead to a lower surface-air temperature. Due to the effects of precipitation, the C–C relation, which means the vapor pressure follows temperature with a rate near 7%/K, is broken.

The quantitative analysis of the dominance of T and R on the variation in E helps understand the response of surface water vapor to temperature in different areas and can provide an advisable reference for the water vapor change under greenhouse warming. Precipitation on land is taken as a case to explain the breaking of the C–C relation between vapor pressure and temperature in some areas. The transport of moist air from wet areas could play a similar role and can also break the C–C relation between E and T. Hence, in some areas, the C–C relation between vapor pressure and temperature may be affected by monsoons, and the relation between water vapor and temperature are influenced by the intensity of monsoons. The specific reasons and physical processes in different regions will be analyzed in future work. The interannual variation in near-surface water vapor pressure, temperature, and relative humidity is studied in this paper. The interannual variation may reflect the sensitivity of water vapor to temperature in different areas. Whether the long-term response of water vapor to temperature also conforms to the interannual characteristics will be also examined in the future work.

Author Contributions: Conceptualization, J.H. and E.L.; methodology, E.L.; software, J.H.; validation, J.H.; formal analysis, J.H. and E.L.; investigation, J.H.; resources, J.H.; data curation, J.H.; writing—original draft preparation, J.H.; writing—review and editing, J.H. and E.L.; visualization, J.H.; supervision, E.L.; project administration, E.L.; funding acquisition, E.L. All authors have read and agreed to the published version of the manuscript.

Funding: This study was supported by the National Natural Science Foundation of China, Grant Number: 41991281. National Key Research and Development Program of China, Grant Number: 2018YFC1507704. Priority Academic Program Development of Jiangsu Higher Education Institutions (PAPD).

Institutional Review Board Statement: Not applicable.

Informed Consent Statement: Not applicable.

Data Availability Statement: The data of precipitable water, precipitation, and the near-surface temperature and dewpoint temperature used in this study were from the ERA5 dataset provided by the ECMWF from the Copernicus Climate Change Service (C3S) Climate Date Store (https://cds.climate.copernicus.eu/cdsapp#!/dataset/reanalysis-era5-single-levels-monthly-means (accessed on 20 July 2022)). The data on precipitation from the CPC (Climate Prediction Center) Merged Analysis of Precipitation (CMAP) are can be achieved on https://www.cpc.ncep.noaa.gov/products/global_precip/html/wpage.cmap.shtml (accessed on 20 July 2022).

Conflicts of Interest: The authors declare no conflict of interest.

References

1. Stewart, R.E.; Leighton, H.G.; Marsh, P.; Moore, G.W.K.; Ritchie, H.; Rouse, W.R.; Soulis, E.D.; Strong, G.S.; Crawford, R.W.; Kochtubajda, B. The Mackenzie GEWEX study: The water and energy cycles of a major North American river basin. *Bull. Am. Meteorol. Soc.* **1998**, *79*, 2665–2684. [CrossRef]
2. Semmler, T.; Jacob, D.; Schlünzen, K.H.; Podzun, R. The water and energy budget of the Arctic atmosphere. *J. Clim.* **2005**, *18*, 2515–2530. [CrossRef]
3. Trenberth, K.E.; Fasullo, J.T. Regional energy and water cycles: Transports from ocean to land. *J. Clim.* **2013**, *26*, 7837–7851. [CrossRef]
4. Mathew, S.S.; Kumar, K.K. On the role of precipitation latent heating in modulating the strength and width of the Hadley circulation. *Theor. Appl. Climatol.* **2019**, *136*, 661–673. [CrossRef]
5. Zhou, T.J.; Yu, R.C. Atmospheric water vapor transport associated with typical anomalous summer rainfall patterns in China. *J. Geophys. Res.* **2005**, *110*, D08104. [CrossRef]
6. Radel, G.; Shine, K.P.; Ptashnik, I.V. Global radiative and climate effect of the water vapour continuum at visible and near-infrared wavelengths. Quart. *J. R. Meteorol. Soc.* **2015**, *141*, 727–738. [CrossRef]
7. Cady-Pereira, K.E.; Shephard, M.W.; Turner, D.D.; Mlawer, E.J.; Clough, S.A.; Wagner, T.J. Improved daytime column-integrated precipitable water vapor from Vaisala radiosonde humidity sensors. *J. Atmos. Oceanic Technol.* **2008**, *25*, 873–883. [CrossRef]
8. Durre, I.; Williams, C.N.; Yin, X.; Vose, R.S. Radiosonde-based trends in precipitable water over the northern hemisphere: An update. *J. Geophys. Res.* **2009**, *114*, D05112. [CrossRef]
9. Dostalek, F.J.; Schmit, T.J. Total precipitable water measurements from GOES sounder derived product imagery. *Weather Forecast.* **2001**, *16*, 573–587. [CrossRef]
10. Deeter, M.N. A new satellite retrieval method for precipitable water vapor over land and ocean. *Geophys. Res. Lett.* **2007**, *34*, L02815. [CrossRef]
11. Radhakrishna, B.; Fabry, F.; Braun, J.J.; Van Hove, T. Precipitable water from GPS over the continental United States: Diurnal cycle, intercomparisons with NARR, and link with convective initiation. *J. Clim.* **2015**, *28*, 2584–2599. [CrossRef]
12. Torri, G.; Adams, D.K.; Wang, H.; Kuang, Z. On the diurnal cycle of GPS-derived precipitable water vapor over Sumatra. *J. Atmos. Sci.* **2019**, *76*, 3529–3552. [CrossRef]
13. Zveryaev, I.I.; Chu, P.S. Recent climate changes in precipitable water in the global tropics as revealed in National Centers for Environmental Prediction/National Center for Atmospheric Research reanalysis. *J. Geophys. Res.* **2003**, *108*, 4311. [CrossRef]
14. Ssenyunzi, R.C.; Oruru, B.; D'ujanga, F.M.; Realini, E.; Barindelli, S.; Tagliaferro, G.; von Engeln, A.; van de Giesen, N. Performance of ERA5 data in retrieving precipitable water vapour over East African tropical region. *Adv. Space Res.* **2020**, *65*, 1877–1893. [CrossRef]
15. Wang, J.X.L.; Gaffen, D.J. Late-twentieth-century climatology and trends of surface humidity and temperature in China. *J. Clim.* **2001**, *14*, 2833–2845. [CrossRef]
16. Dai, A. Recent climatology, variability, and trends in global surface humidity. *J. Clim.* **2006**, *19*, 3589–3606. [CrossRef]
17. Willett, K.M.; Jones, P.D.; Gillett, N.P.; Thorne, P.W. Recent changes in surface humidity: Development of the HadCRUH dataset. *J. Clim.* **2008**, *21*, 5364–5383. [CrossRef]
18. Isaac, V.; van Wijngaarden, W.A. Surface water vapor pressure and temperature trends in North America during 1948–2010. *J. Clim.* **2012**, *25*, 3599–3609. [CrossRef]
19. Wallace, J.M.; Hobbs, P.V. *Atmospheric Science: An Introductory Survey*; Elsevier Science: Amsterdam, The Netherlands, 2006.
20. Lu, E.; Zeng, X. Understanding different precipitation seasonality regimes from water vapor and temperature fields: Case studies. *Geophys. Res. Lett.* **2005**, *32*, L22707. [CrossRef]
21. Lu, E. Understanding the effects of atmospheric circulation in the relationships between water vapor and temperature through theoretical analyses. *Geophys. Res. Lett.* **2007**, *34*, L14811. [CrossRef]
22. Reber, E.E.; Swope, J.R. On the correlation of the total precipitable water in a vertical column and absolute humidity at the surface. *J. Appl. Meteorol.* **1972**, *11*, 1322–1325. [CrossRef]
23. Viswanadham, Y. The relationship between total precipitable water and surface dew point. *J. Appl. Meteor.* **1981**, *20*, 3–8. [CrossRef]
24. Liu, W.T. Statistical relation between monthly mean precipitable water and surface-level humidity over global oceans. *Mon. Weather Rev.* **1986**, *114*, 1591–1602. [CrossRef]

25. Hsu, S.A.; Blanchard, B.W. The relationship between total precipitable water and surface-level humidity over the sea surface: A further evaluation. *J. Geophys. Res.* **1989**, *94*, 14539–14545. [CrossRef]
26. Gaffen, D.J.; Elliott, W.P.; Robock, A. Relationships between tropospheric water vapor and surface temperature as observed by radiosondes. *Geophys. Res. Lett.* **1992**, *19*, 1839–1842. [CrossRef]
27. Sun, D.Z.; Held, I.M. A comparison of modeled and observed relationships between interannual variations of water vapor and temperature. *J. Clim.* **1996**, *9*, 665–675. [CrossRef]
28. Bauer, M.; Genio, A.D.; Lanzante, J.R. Observed and simulated temperature-humidity relationships: Sensitivity to sampling and analysis. *J. Clim.* **2002**, *15*, 203–215. [CrossRef]
29. Mears, C.A.; Santer, B.D.; Wentz, F.J.; Taylor, K.E.; Wehner, M.F. Relationship between temperature and precipitable water changes over tropical oceans. *Geophys. Res. Lett.* **2007**, *34*, L24709. [CrossRef]
30. O'Gorman, P.A. Sensitivity of tropical precipitation extremes to climate change. *Nat. Geosci.* **2012**, *5*, 697–700. [CrossRef]
31. Chung, E.S.; Soden, B.; Sohn, B.J.; Shi, L. Upper-tropospheric moistening in response to anthropogenic warming. *Proc. Natl. Acad. Sci. USA* **2014**, *111*, 11636–11641. [CrossRef]
32. Collins, M.; Knutti, R.; Arblaster, J.; Dufresne, J.L.; Fichefet, T.; Friedlingstein, P.; Gao, X.; Gutowski, W.J.; Johns, T.; Krinner, G.; et al. Long-term climate change: Projections, commitments and irreversibility. In *Climate Change 2013: The Physical Science Basis*; Cambridge University Press: New York, NY, USA, 2013; pp. 1029–1136.
33. Vicente-Serrano, S.M.; Azorin-Molina, C.; SanchezLorenzo, A.; Morán-Tejeda, E.; Lorenzo-Lacruz, J.; Revuelto, J.; López-Moreno, J.I.; Espejo, F. Temporal evolution of surface humidity in Spain: Recent trends and possible physical mechanisms. *Clim. Dyn.* **2014**, *42*, 2655–2674. [CrossRef]
34. Vicente-Serrano, S.M.; Nieto, R.; Gimeno, L.; Azorin-Molina, C.; Drumond, A.; El Kenawy, A.; Dominguez-Castro, F.; Tomas-Burguera, M.; Peña-Gallardo, M. Recent changes of relative humidity: Regional connections with land and ocean processes. *Earth Syst. Dyn.* **2018**, *9*, 915–937. [CrossRef]
35. Lu, E.; Takle, E.S.; Manoj, J. The relationships between climatic and hydrological changes in the upper Mississippi River basin: A SWAT and multi-GCM study. *J. Hydrometeor.* **2010**, *11*, 437–451. [CrossRef]
36. Lu, E.; Ding, Y.; Zhou, B.; Zou, X.; Chen, X.; Cai, W.; Zhang, Q.; Chen, H. Is the interannual variability of summer rainfall in China dominated by precipitation frequency or intensity? An analysis of relative importance. *Clim. Dyn.* **2016**, *47*, 67–77. [CrossRef]
37. Lu, E.; Tu, J. Relative importance of surface-air temperature and density to interannual variations in monthly surface atmospheric pressure. *Int. J. Climatol.* **2020**, *41*, E819–E831. [CrossRef]
38. Tu, J.; Lu, E. Relative importance of water vapor and air temperature in the interannual variation of the seasonal precipitation: A comparison of the physical and statistical methods. *Clim. Dyn.* **2020**, *54*, 3655–3670. [CrossRef]
39. Hersbach, H.; Bell, B.; Berrisford, P.; Hirahara, S.; Horányi, A.; Muñoz-Sabater, J.; Nicolas, J.; Peubey, C.; Radu, R.; Schepers, D.; et al. The ERA5 global reanalysis. *Q. J. R. Meteorol. Soc.* **2020**, *146*, 1999–2049. [CrossRef]
40. Xie, P.; Arkin, P.A. Global precipitation: A 17-year monthly analysis based on gauge observations, satellite estimates, and numerical model outputs. *Bull. Am. Meteorol. Soc.* **1997**, *78*, 2539–2558. [CrossRef]
41. Peixoto, J.P.; Oort, A.H. *Physics of Climate*; American Institute of Physics: New York, NY, USA, 1992; Volume 520.
42. Gillett, N.P.; Kell, T.D.; Jones, P.D. Regional climate impacts of the Southern Annular Mode. *Geophys. Res. Lett.* **2006**, *33*, L23704. [CrossRef]
43. Soden, B.J. The sensitivity of the tropical hydrological cycle to ENSO. *J. Clim.* **2000**, *13*, 538–549. [CrossRef]